A novel hybrid terpyridine–pyrimidine ligand and the supramolecular structures of two of its complexes with Zn(II) and acetylacetonato: The underlying role of non-covalent π···π contacts and C–H···X(O, N, π) hydrogen bonds

Juan Granifo [a,*], Rubén Gaviño [b], Eleonora Freire [c,d], Ricardo Baggio [c]

[a] Departamento de Ciencias Químicas y Recursos Naturales, Facultad de Ingeniería y Ciencias, Universidad de La Frontera, Casilla 54-D, Temuco, Chile
[b] Instituto de Química, Universidad Nacional Autónoma de México, Cd. Universitaria, Circuito Exterior Coyoacán, 04510 México, DF, Mexico
[c] Departamento de Física, Comisión Nacional de Energía Atómica, Av. Gral Paz 1499, 1650 San Martín, Pcia. de Buenos Aires, Argentina
[d] Escuela de Ciencia y Tecnología, Universidad Nacional de San Martín, Buenos Aires, Argentina

HIGHLIGHTS

- A novel hybrid terpyridine–pyrimidine ligand (**L1**) was synthesized.
- The reaction of **L1** with Zn(acac)$_2$ gives simultaneously **1** and **2**.
- **1** and **2** present C–H···N bonds generating planar 2D aromatic structures.
- The spacings between the 2D arrays strongly suggests a π···π linkage among them.

GRAPHICAL ABSTRACT
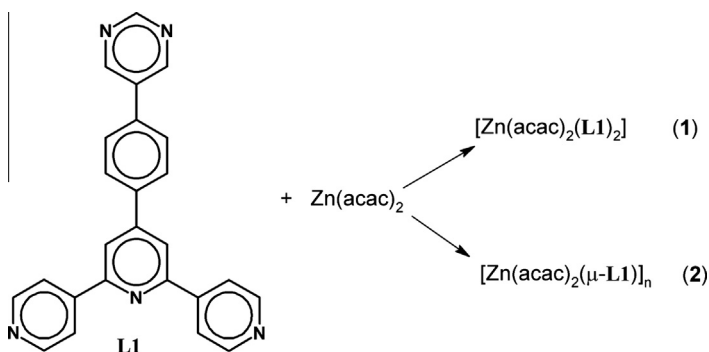
ARTICLE INFO

ABSTRACT

The novel 4′-[4-(pyrimidin-5-yl)phenyl]-4,4′:6′,2″-terpyridine (**L1**) ligand reacts with Zn(acac)$_2$ (acac = acetylacetonato) to give the monomeric complex [Zn(acac)$_2$(**L1**)$_2$] (**1**) and the coordination polymer [Zn(acac)$_2$(μ-**L1**)]$_n$ (**2**). The structure of **1** consists of a Zn(II) cation sitting on an inversion centre, surrounded by a slightly elongated octahedral environment, defined by two *trans* N(4-pyridyl) atoms from a pair of mondentate **L1** ligands, and four O atoms from two chelating acac anions. The polymeric structure of **2** presents a similar though non-symmetric Zn(acac)$_2$ unit, since the two coordinated N atoms come from two different donor moieties of **L1**: the 4-pyridyl and the pyrimidinyl. Both compounds present weak C–H···N contacts generating 2D aromatic structures, complemented by π···π contacts plane-stacking giving raise to 3D structures and further stabilized by C–H···O and C–H···π interactions.

© 2014 Elsevier B.V. All rights reserved.

1. Introduction

The large number of studies of the coordination chemistry of the tridentate ligand 2,2′:6′,6″-terpyridine and its 4′-substituted derivatives has been centered mainly in its action as chelating ligands [1–3], i. e., where they present a convergent disposition of its N,N′,N″ donor atoms to link the metal atoms. More recently, as a further exploration in this type of metal-binding domains, the divergent 4,4″ isomers and pyridyl-substituted in the 4′-position have been used [4–11]. Indeed, to the best of our knowledge, in

* Corresponding author. Tel.: +56 045 2325434.
E-mail address: juan.granifo@ufrontera.cl (J. Granifo).
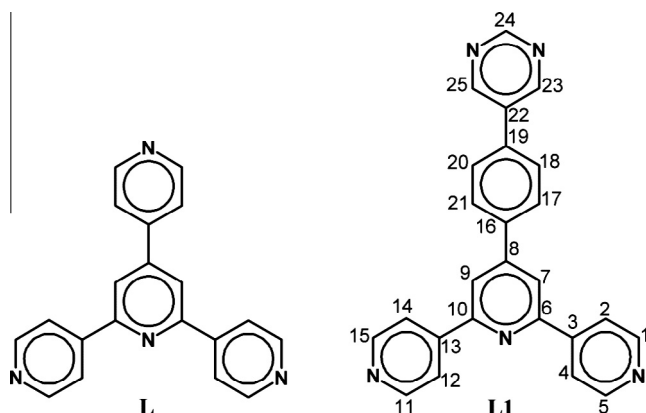
Scheme 1. The sketches of the ligands **L** and **L1**. For **L1** the numbering of carbon atoms (hydrogen atoms where correspond) is indicated.

all the reported examples only the 4′-(4-pyridyl)-4′,2′:6′,4″-terpyridine ligand (**L**, Scheme 1) has been tested. The divergent nature of **L** has allowed to connect metal centers acting either as bidentate-bridging (using the 4,4″pyridyl groups to give infinite chain structures [4–6] or a 3D network structure [7]) or as tridentate (using the three external 4-pyridyl groups to engage 3D structural motifs [8] or molecular capsules [9,10]). In addition, a polymeric Cu(II) compound with a protonated HL$^+$ ligand has been reported [11] as well as two coordination polymers containing a chloro derivate of **L** [9]. It is relevant to mention here that the coordination polymer [Co(acac)$_2$(μ-L)]$_n$ [4] is the sole example where the *acac* and **L** ligands coexist, with the last one presenting a symmetric nature to form the bridge by using the pyridyl-nitrogen atoms N and N″.

In this work, as an extension of the studies of bonding and supramolecular properties of the 4,4″ divergent terpyridine-based ligands, we decided to replace in **L** its pyridyl portion localized in the 4′-position by another containing the pyrimidinyl fragment

to afford the related **L1** ligand (Scheme 1). It was expected that the inclusion of a N-donor substituent like the pyrimidine moiety can act not only as a metal coordination site, but also to enable the diversification of the types of non-covalent interactions present, such as hydrogen bonding, π–π stacking, etc. Under these expectations, the coordinating properties of **L1** were tested by reacting it with Zn(acac)$_2$ to afford simultaneously the molecular complex **1**, with **L1** as a monodentate N-pyridyl donor ligand, and the polymer **2**, with **L1** as an asymmetric-bidentate bridging ligand employing N atoms from the pyridyl and pyrimidinyl fragments.

2. Experimental

The solvents were purchased from commercial sources and used without further purification. The compound Zn(acac)$_2$ was obtained from Aldrich. Infrared spectra were recorded using KBr plates on a Bruker Tensor 27 FT-IR spectrometer. An Exeter Analytical CE-440 elemental analyser was used for microanalysis (C, H, N). ^{1}H and ^{13}C NMR spectra were recorded on a Bruker Avance 300 MHz NMR instrument.

2.1. Synthesis of 4′-[4-(pyrimidin-5-yl)phenyl]-4,2′:6′,4″-terpyridine (**L1**)

L1 was prepared by using the one-pot method of Hanan and Wang [12]. 4-Acetylpyridine (0.61 g, 5.0 mmol) was added to a solution of 4-(pyrimidin-5-yl)benzaldehyde (0.46 g, 2.5 mmol) in EtOH (20 mL). After stirring for 0.25 h, KOH pellets (0.28 g, 5.0 mmol) were added. The resulting solution was stirred at room temperature over a period of 6 h, then an excess of aqueous NH$_3$ (8.6 mL, 25%, 115 mmol) was added and stirring was continued for further 24 h. The solid was filtered off and washed with water (5 × 10 mL) and with ethanol (3 × 10 mL). The product was dissolved in CHCl$_3$ (20 mL) and the addition of methanol (60 mL)

Table 1
Crystal data and refinement parameters for **1** and **2**.

Compound	1	2
Crystal data		
Chemical formula	C$_{60}$H$_{48}$N$_{10}$O$_4$Zn	C$_{35}$H$_{31}$N$_5$O$_4$Zn
M_r	1038.45	651.02
Crystal system, space group	Triclinic, $P-1$	Triclinic, $P-1$
Temperature (K)	295	295
a, b, c (Å)	11.0116 (4), 11.3556 (6), 11.4396 (4)	10.8123 (3), 11.1869 (4), 14.1734 (5)
α, β, γ (°)	115.612 (4), 91.818 (3), 104.204 (4)	66.837 (2), 88.609 (3), 77.171 (3)
V (Å^3)	1234.82 (11)	1533.02 (10)
Z	1	2
Radiation type	Mo Kα	Mo Kα
μ (mm^{-1})	0.56	0.85
Crystal size (mm)	0.32 × 0.24 × 0.08	0.36 × 0.12 × 0.10
Data collection		
Diffractometer	Oxford Diffraction Gemini CCD S Ultra diffractometer	Oxford Diffraction Gemini CCD S Ultra diffractometer
Absorption correction	Multi-scan *CrysAlis PRO*, Oxford Diffraction (2009)	Multi-scan *CrysAlis PRO*, Oxford Diffraction (2009)
T_{min}, T_{max}	0.85, 0.96	0.88, 0.92
No. of measured, independent and observed [$I > 2\sigma(I)$] reflections	14711, 5743, 4901	36853, 7399, 6242
R_{int}	0.025	0.027
$(\sin\theta/\lambda)_{max}$ (Å^{-1})	0.679	0.679
Refinement		
$R[F^2 > 2\sigma(F^2)]$, $wR(F^2)$, S	0.037, 0.098, 1.04	0.031, 0.081, 1.04
No. of reflections	5743	7399
No. of parameters	342	410
No. of restraints	0	0
H-atom treatment	H-atom parameters constrained	H-atom parameters constrained
$\Delta\rangle_{max}, \Delta\rangle_{min}$ (e Å^{-3})	0.25, −0.26	0.24, −0.28

Table 2
Selected bond lengths (Å) and bond angles (°) for **1** and **2**.

(a) Compound **1**			
Zn1–O12	2.0623 (12)	Zn1–N11	2.2505 (13)
Zn1–O22	2.0806 (13)		
O12–Zn1–O22	89.18 (5)	O12–Zn1–N11	90.78 (5)
O22–Zn1–N11	89.31 (5)		
(b) Compound **2**			
Zn1–O13	2.0294 (11)	Zn1–O22	2.0596 (12)
Zn1–O12	2.0375 (11)	Zn1–N11	2.2182 (12)
Zn1–O23	2.0532 (12)	Zn1–N41[i]	2.3860 (13)
O13–Zn1–O12	174.44 (4)	O23–Zn1–N11	91.86 (5)
O13–Zn1–O23	89.69 (5)	O22–Zn1–N11	92.04 (5)
O12–Zn1–O23	89.53 (5)	O13–Zn1–N41[i]	86.76 (5)
O13–Zn1–O22	90.88 (5)	O12–Zn1–N41[i]	87.72 (5)
O12–Zn1–O22	89.52 (5)	O23–Zn1–N41[i]	89.23 (5)
O23–Zn1–O22	176.04 (4)	O22–Zn1–N41[i]	86.89 (5)
O13–Zn1–N11	92.42 (5)	N11–Zn1–N41[i]	178.64 (5)
O12–Zn1–N11	93.11 (5)		

Symmetry code: (i) $x - 1$, y, $z + 1$.

afforded a crystalline solid, which was washed with methanol (3 × 10 mL) (yield: 0.42 g, 43%). Analysis calculated for $C_{25}H_{17}N_5$: C 77.50, H 4.42, N 18.08%; found: C 77.40, H 4.38, N 18.15%. ^{13}C-PND and ^{13}C-DEPT NMR (75 MHz, CDCl$_3$, 298 K): δ = 158.0 (CH), 155.6 (Cquat), 154.9 (CH), 150.7 (CH), 150.1 (Cquat), 145.9 (Cquat), 138.7 (Cquat), 135.6 (Cquat), 133.4 (Cquat), 128.3 (CH), 127.9 (CH), 121.2(CH), 118.8(CH). ^{1}H NMR (300 MHz, CDCl$_3$, 298 K): δ = 9.25 (s, 1H), 9.02 (s, 2H), 8.79 (AA′, 4H, J = 4.5 Hz), 8.07 (BB′, 4H, J = 4.5 Hz), 8.06 (s, 2H), 7.90 (AA′, 2H, 8.1 Hz), 7.78 (BB′, 2H, 8.1 Hz). IR (KBr, cm^{-1}): 2848, 1594, 1535, 1389, 1129, 997, 810.

2.2. Synthesis of [Zn(acac)$_2$(**L1**)$_2$] (**1**) and [Zn(acac)$_2$(μ-**L1**)]$_n$ (**2**)

To a hot solution (using an oil bath at 57–60 °C) of **L1** (7.6 mg, 0.020 mmol) in MeOH (6.0 mL) contained in a closed volumetric flask (10 mL) was added an excess of Zn(acac)$_2$ (65.0 mg, 0.25 mmol). The resultant solution was heated in the oil bath for 15 h. A mixture of needle-like and block-like colorless crystals were obtained after the removal of the hot solvent, washing with MeOH (4 × 4 mL) and diethyl ether (2 × 4 mL) and dried in the air. From the final product (8.2 mg), crystals suitable for single crystal X-ray analysis were separated by hand. Scarse material

was obtained for analysis of the bulk sample and the spectroscopic measurements evidence the mixture of the two compounds.

2.3. X-ray crystallography

Crystal Data were collected on a Oxford Gemini CCD S Ultra diffractometer at room temperature using Mo Kα radiation (λ = 0.71073 Å). The structure was solved by direct methods and refined by full-matrix least squares on F^2 using the SHELXS-97 software [13,14]. All non-hydrogen atoms were refined anisotropically. Hydrogen atoms were found in a difference Fourier but further idealized. The structural analysis was performed with the help of the multipurpose PLATON program [15].

Data collection and refinement parameters are summarized in Table 1, while selected bond lengths and angles are presented in Table 2. The molecular representations shown in the figures were generated using XP in the SHELXTL package [14] and MERCURY [16]. Crystallographic data (excluding structure factors) for the structures in this paper have been deposited with the Cambridge Crystallographic Data Centre as supplementary publication No. CCDC 970229-970230. Copies of the data can be obtained, free of charge, on application to CCDC, 12 Union Road, Cambridge CB2 1EZ, UK, (fax: +44 1223 336033 or e-mail: deposit@ccdc.cam.ac.uk).

3. Results and discussion

3.1. The NMR spectra of **L1** (performed through Correlation Spectroscopy (COSY), Distortionless Enhancement of Polarisation Transfer (DEPT) and Proton Noise Decoupled (PND))

The NMR results in CDCl$_3$ solution of the **L1** ligand are in good agreement with the expected molecular structure (Scheme 1 and Section 2.1). Thus, the ^{13}C NMR spectrum shows 13 signals exclusively for sp^2 carbon atoms, the carbon multiplicity was determined by ^{13}C-DEPT experiment: six signals are due to quaternary carbons 155.6 (C6/C10), 150.1 (C8), 145.9 (C3/C13), 138.7 (C16), 135.6 (C19), 133.4 (C22) and seven due to CH carbons 158.0 (C24), 154.9 (C23/C25), 150.7 (C1/C5/C11/C15), 128.3 (C18/C20), 127.9 (C17/C21), 121.2 (C2/C4/C12/C14) and 118.8 (C7/C9). Similarly, the ^{1}H NMR is characterized for a low field singlet (9.25 ppm) and a second singlet (9.02 ppm) due to the pyrimidine protons H24 and H23/25, respectively. The four phenyl protons can
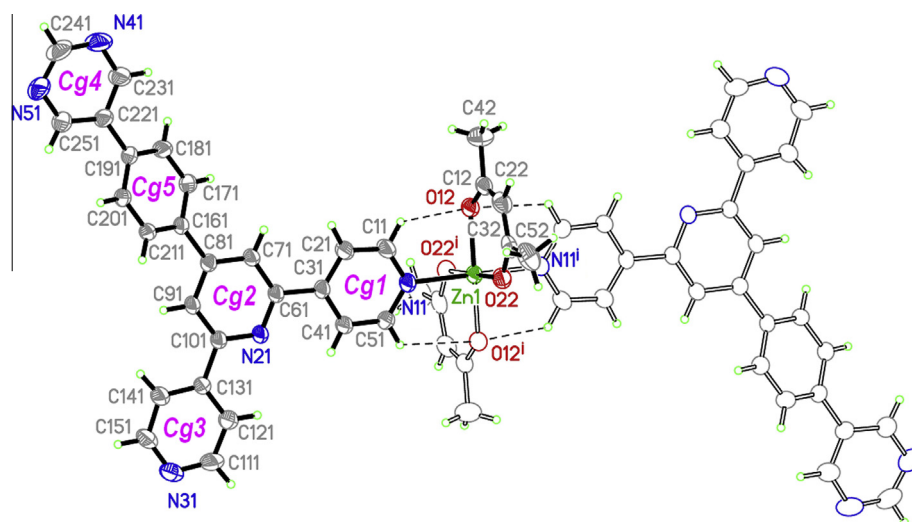

Fig. 1. Molecular diagram of **1**, with 40% displacement ellipsoids, showing atom and ring labeling. Full (empty) bonds and atoms denote the independent (symmetry related) part of the structure. In broken bonds the intramolecular C–H⋯O hydrogen bonds. Symmetry code: (i) $-x + 1$, $-y + 1$, $-z + 1$.

Table 3
Relevant hydrogen-bonds (Å, °) found in **1** and **2**.

D–H···A	D–H	H···A	D···A	D–H···A
(a) Compound **1**				
C11–H11···O12	0.93	2.50	3.104 (2)	123
C51–H51···O12^i	0.93	2.53	3.114 (2)	121
C21–H21···N31^{ii}	0.93	2.70	3.569 (3)	156
C251–H251···N51^{iii}	0.93	2.72	3.601 (3)	159
C231–H231···O22^{iv}	0.93	2.61	3.393 (4)	142
C181–H181···O22^{iv}	0.93	2.72	3.641 (4)	170
C52–H52B···Cg5^v	0.96	3.28	3.900 (4)	124
(b) Compound **2**				
C51–H51···O13	0.93	2.49	3.102 (2)	124
C231–H231···O12^{ii}	0.93	2.48	3.083 (2)	122
C11–H11···O12	0.93	2.64	3.210 (3)	120
C241–H241···O13^{ii}	0.93	2.64	3.203 (2)	119
C21–H21···N31^{iii}	0.93	2.69	3.371 (2)	131
C41–H41···O22^{iv}	0.93	2.48	3.382 (2)	163
C211–H211···O22^{iv}	0.93	2.68	3.603 (2)	172
C141–H141···Cg5^v	0.93	2.80	3.446 (2)	128
C52–H52C···Cg3^{vi}	0.96	3.12	3.842 (3)	133

Symmetry codes: (i) −x + 1, −y + 1, −z + 1; (ii) x + 1, y, z; (iii) −x, −y − 1, −z − 2; (iv) x, y − 1, z − 1; (v) −x + 1, −y + 1, −z. Ring code: Cg5, C161 → C211.
Symmetry codes: (ii) x + 1, y, z − 1; (iii) −x, −y + 2, −z; (iv) −x + 1, −y + 1, −z + 1; (v) −x + 1, −y + 2, −z; (vi) x, y − 1, z + 1. Ring code: Cg2, N21,C61 → C101; Cg5, C161 → C211.

Table 4
π···π contacts in **1** and **2** (Å, °).

Group 1···Group 2	ccd (Å)	da (°)	ipd (Å)
(a) Compound **1**			
Cg1···Cg4^{vi}	3.629 (2)	2.12 (14)	3.565 (11)
Cg1···Cg3^{vii}	4.057 (2)	9.12 (19)	3.59 (18)
Cg3···Cg4^{viii}	3.946 (2)	8.89 (18)	3.66 (6)
(b) Compound **2**			
Cg2···Cg2^{vii}	3.8631 (10)	0	3.6262 (7)
Cg3···Cg4^{viii}	3.8633 (12)	20.92 (9)	3.4 (3)
Cg4···Cg5^{ix}	3.9643 (11)	29.29 (9)	3.5 (4)

Symmetry codes: (vi) x, 1 + y, 1 + z; (vii) −x, −y, −z; (viii) −x, −y, −1 − z. Ring code: Cg1: N11,C11 → C51; Cg3: N31, C111 → C151, Cg4: N41, N51, C221 → C251.
Symmetry codes: (vii) 1 − x, 2 − y, −z; (viii) −1 + x, y, z;(ix) 2 − x, 1 − y, −z; Ring code: Cg2, N21,C61 → C101, Cg3, N31,C111 → C151; Cg4, N41,N51, C221 → C251; Cg5, C161 → C211.ccd: center-to-center distance; da: dihedral angle between rings; ipd: interplanar distance, or (mean) distance from one plane to the neighboring centroid.

3.2. Coordination geometry, bonding and non-covalent contacts in the monomeric complex 1

The single-crystal X-ray structure of **1** (Fig. 1 and Table 2) reveals a monomeric species with a sixfold coordinated Zn cation on an inversion centre, bound to a monodentate **L1** ligand, through a 4-pyridyl N atom, a chelating-bidentate *acac*-κ^{2}O,O′ anion, through both O atoms, and their two centrosymmetric images. The environment of Zn1 is an octahedron, with the two chelating *acac* ligands defining the ZnO$_4$ base (Zn–O range: 2.0623 (12)– 2.0806 (13) Å) and both coordinated N(4-pyridyl) atoms occupying the apical sites, with slightly elongated bonds of Zn–N: 2.2505 (13) Å. Angular deformations, in turn, are quite small (cis-angles
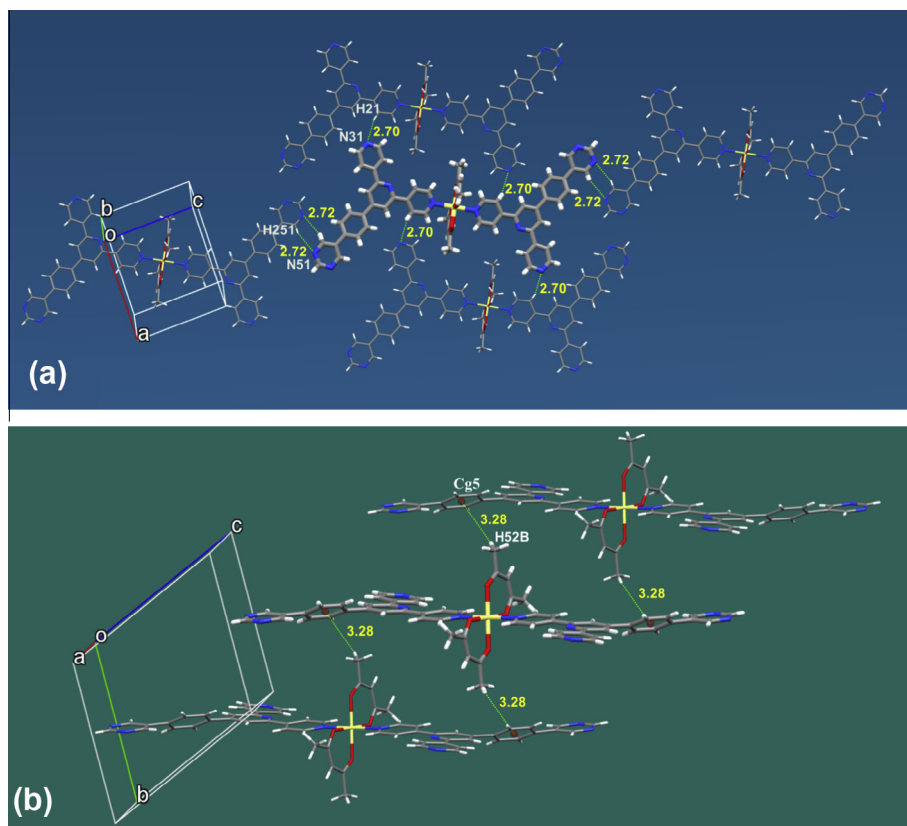
be readily distinguished by the characteristic AA′BB′ pattern for H17/H21 (7.90 ppm) and H18/H20 (7.78 ppm). The two protons of the central pyridine ring H7/H9 appear as a singlet (8.06 ppm). The eight protons of the two 4-pyridyl rings in and positions show an AA′BB′ pattern for H1/H5/H11/H15 (8.79 ppm) and for H2/H4/ H12/H14 (8.07 pm).

Fig. 2. Packing diagram of **1**. **(a):** The 2D substructure formed by the intermolecular C–H···N hydrogen bonds. One central monomeric unit is presented surrounded by the neighboring species. **(b)** CH(methyl)/π(Cg5) hydrogen bond.
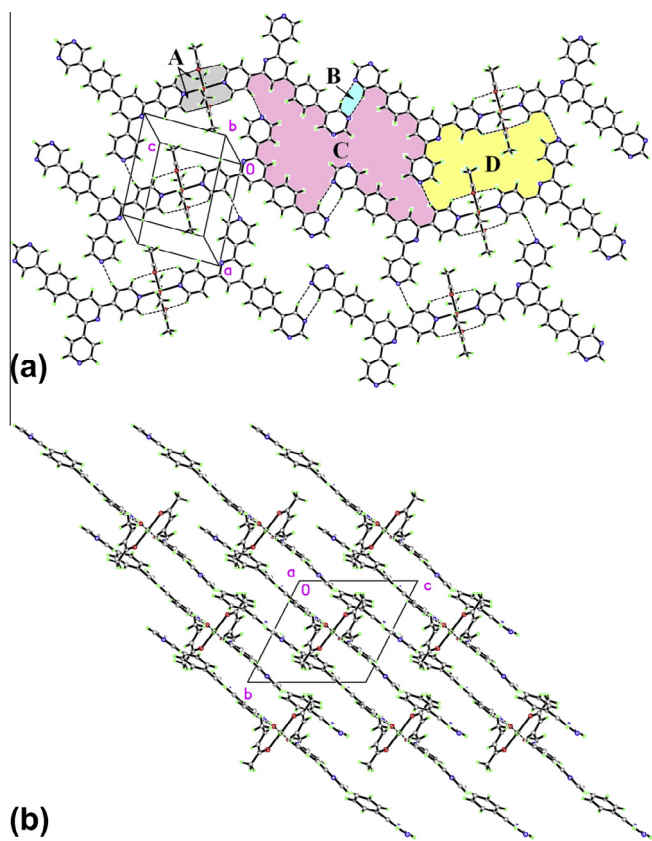
Fig. 3. Packing diagram of **1**. (a) The hydrogen bonded 2D substructure defined the intramolecular C–H···O motifs (rings A) and by intermolecular C–H···N motifs (rings B–D). For ring definitions, see text. (b) The stacking of planes, as described in the text.

range: O–Zn–O: 90 ± 0.82 (5)°, O–Zn–N: 90 ± 0.69 (5)°; trans-angles being exactly 180° due to symmetry constraints). Also due to these symmetry limitations the basal plane is perfectly planar, with the apical bond being almost perpendicular to the plane, at 179.0 (2)°. The **L1** ligand, in turn, presents an essentially planar substructure made up of the four N-containing groups: rings 1 → 4 (See Fig. 1 for ring labeling) adopt a collective flattened disposition, with a mean deviation from the L.S. plane of 0.0637 Å, and a maximum departure of 0.141 (2) Å for C111. The central phenyl ring 5, however, protrudes significantly from this planar geometry, through a rotation of 26.8 (2)° around the

C161···C221 axis. Finally, *acac* moieties do not present any significant deviation from commonly accepted values both in distances as in angles.

In **1** there are many non-covalent interactions of varied type and strength, which are presented in Table 3a (H-bonding) and Table 4a (π···π interactions). For the sake of simplicity, in what follows we shall use a shorthand notation, viz., "T$n(m)$" to denote "Table n (mth entry)".

The packing of structure **1** is characterized by the presence of a 2D substructure based on intramolecular C–H···O (Fig. 1) and intermolecular C–H···N (Fig. 2a) hydrogen bonds. The intramolecular C–H···O contacts involve H atoms from the coordinated 4-pyridyl groups and the O atoms from the *acac*, T3a(1,2) (Fig. 1), generating a S(5) ring (A in Fig. 3a; for a survey on Graph Set nomenclature of H-bonding loops, see Etter [17] and Bernstein et al. [18]), which serve to further stabilize the coordination polyhedra. Regarding intermolecular C–H···N interactions, they are weak but they give rise anyway to a well defined structure, and comprise the N atom of the non-coordinated 4-pyridyl group, T3a(3), and only one N atom of the pyrimidinyl group, T3a(4). The motifs that include the two different C–H···N contacts are shown in Fig. 3a, and by using the graph notation we find three different types of rings, R_2^2 (6) (B in Fig. 3a), R_4^4 (58) (C) and R_6^6 (32) (D). Therefore, the resultant of all non-covalent interactions indicated above define a planar 2D array of aromatic rings parallel to (0 3 $\bar{2}$), characterized by a number of H-bonding rings of quite different size and shape. This 2D array build up a parallel stacking of planes (Fig. 3b), with interplanar spacings of 3.59 Å (the d(0 3 $\bar{2}$) spacing)), which strongly suggests a π···π linkage between planes. Under this premise, the observed array should perhaps be described as an overall interaction of delocalized electronic density clouds distributed along the aromatic system, better than defined in terms of individual π···π interactions, with a large dispersion of inter-centroid distances and slippages (nonetheless reported in T4a(1,2,3). Further support for this argument can be found in the extreme planarity of this 2D substructure (RMS deviations from the planes defined by C and N atoms: 0.15 Å), difficult to sustain without some sort of extended interaction. Additional support to this tentative proposal could be found attempting theoretical studies, e.g., as those obtained for some zinc-organic complexes [19–22], by using quantum chemical methods of the density functional theory and of the electron density topological analysis.

In addition to the generalized π···π bonds, interplanar cohesion is also sustained by some localized C–H···O (T3a(5,6)) and C–H···π (T3a(7)) interactions, which also provide some clues for the already
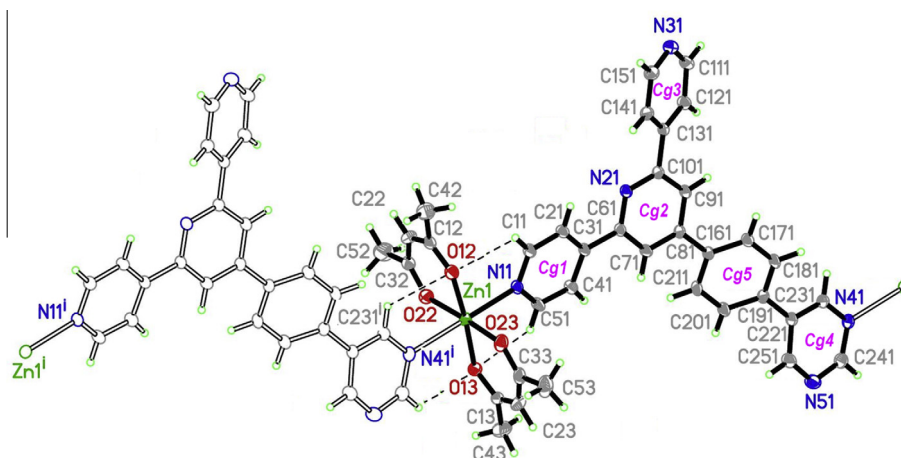

Fig. 4. Molecular diagram of **2**, with 40% displacement ellipsoids, showing atom and ring labeling. Full(empty) bonds and atoms denote the independent (symmetry related) part of the structure. In broken bonds the intramolecular C–H···O bonds. Symmetry code: (i) $x - 1$, y, $z + 1$.
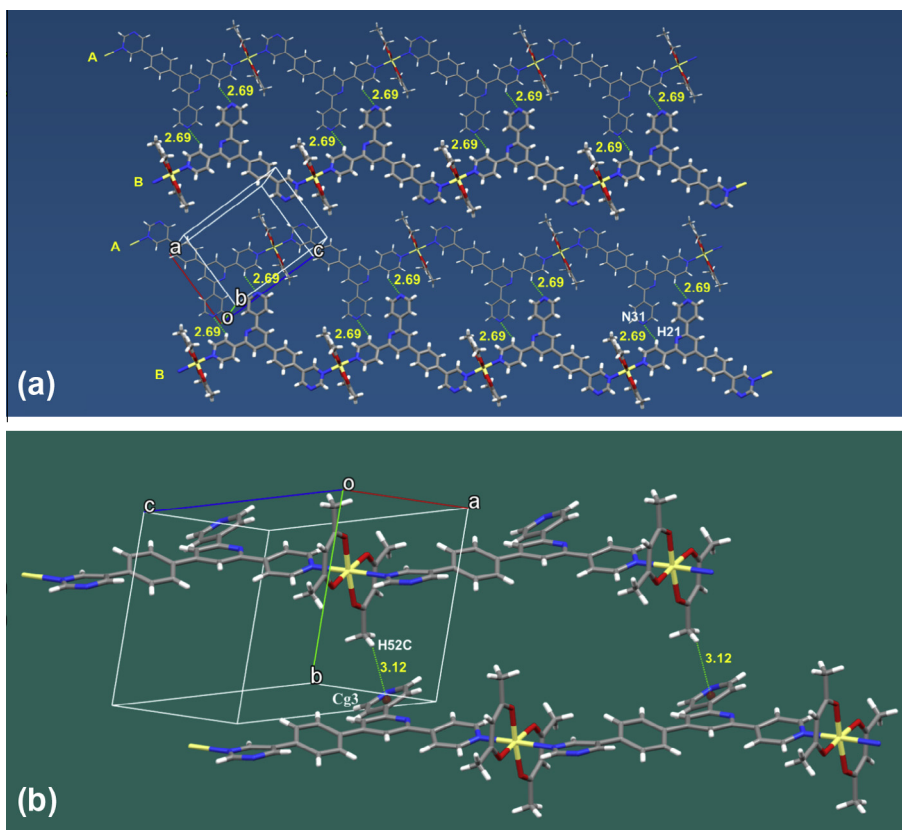
Fig. 5. Packing diagram of **2**. **(a):** The 2D substructure formed by the intermolecular C–H···N hydrogen bonds. A and B are strands of inversion related [$\bar{1}$ 0 1] chains. **(b):** The CH(methyl)/π(Cg3) hydrogen bond.
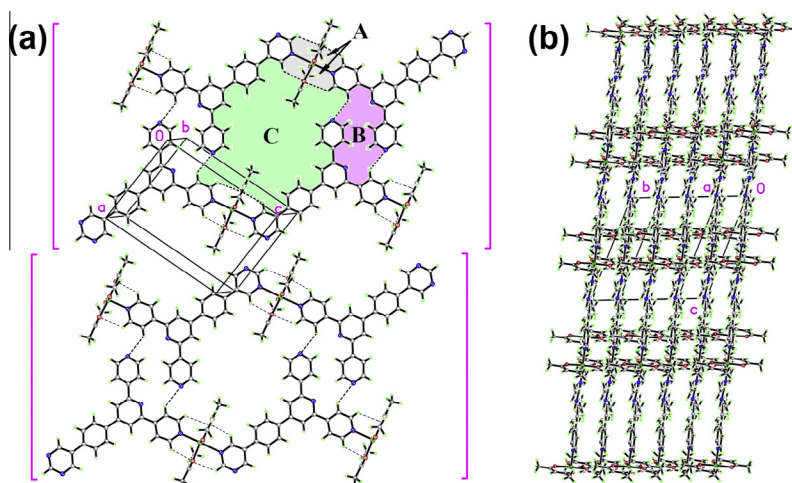

Fig. 6. Packing diagram of **2**. **(a):** The band substructure defined by C–H···N bonds. For ring definitions, see text. **(b):** The stacking of planes, as described in the text.

mentioned rotational deviation of the phenyl ring 5 out of the overall mean plane. More specifically, there are two interactions engaged in the torsion: one is a CH(phenyl)/O(*acac*) connection, C181H181···O22, and the remaining one have the *acac*-CH$_3$ group as H-bond donor directed towards the phenyl ring (C52–H52B···Cg5; Fig. 2b) [23]. Even if these interactions are particularly weak (H···O and H···π distances are beyond commonly accepted values for relevant contacts) the rotational barrier for these movements are sufficiently low as to make the effect of these interactions noticeable.

3.3. Coordination geometry and bonding in the coordination polymer **2**

The polymeric structure **2** (Fig. 4 and Table 2) is compared here with the already described structure **1**. In this regard, it exhibits a sixfold coordinated Zn cation, but now laying on a general position and bound to two bidentate bridging **L1** ligands related by a [−110] translation. In each *trans* 4 + 2 environment of the Zn centres, the basal plane is defined by two (now independent) κ^{2}O,O′ chelating-bidentate *acac* anions and the axial positions are, in this case, occupied by two asymmetric N atoms: one from a 4-pyridyl group

and the other one from a pyrimidinyl group. The environment of the Zn atom in **2** is less regular than its counterpart in **1**, due to the lack of symmetry, though it preserves the same general trend (basal Zn–O range: 2.0294 (11)–2.0596 (12) Å; apical Zn–N range: 2.2182 (12)–2.3860 (13) Å. Angular deformations are also larger, (cis-angles range: O–Zn–O: 90 ± 0.88 (5)°, O–Zn–N: 90 ± 3.24 (5)°; trans-angles: O–Zn–O: 174.44 (4), 176.04 (4)°, N–Zn–N: 178.64 (5)°). The basal plane is very nearly planar, with a mean deviation of ±0.014 (2) Å for all oxygen atoms and leaving the cation 0.085 (4) Å aside. Apical bonds deviate little from the plane normal (0.4 and 1.3°, respectively). The structure of the **L1** ligand in **2** is significantly more deformed than in **1** through rotations of many of its constitutive rings: only rings 2 and 4 remain roughly in a plane (mean deviation from the L.S. plane of 0.069 (3) Å, and a maximum departure of 0.125 (2) Å for C251). The remaining three rings depart significantly from this basic framework through rotations around the single C–C bonds (viz., ring 1, by 14.8 Å, ring 3 by 24.1 Å and ring 5 by 25.1 Å). Similarly to **1**, *acac* ligands in **2** show the standard values both in distances as in angles.

The type of non-covalent interactions in **2** (Tables 3b and 4b and Figs. 4, 5a and b, 6a and b) are similar to those in **1**. Thus, in **2** the intramolecular C–H···O contacts are present, T3b(1,2,3,4) (Fig. 4), but in this case by using hydrogen atoms of the coordinated pyridyl and pyrimidinyl groups to contact the *acac* oxygens atoms, displaying a S(5) motif (A in Fig. 6a). Likewise, the intermolecular C–H···N interactions appear defining a planar 2D array (Fig. 5a), but instead of the two contacts of **1** here there is only one that involves the N atom of the uncoordinated 4-pyridyl group, T3b(5), and its effect is to link pairs of neighboring, inversion related [$\bar{1}$ 0 1] chains, defining bands of aromatic rings (shown in brackets in Fig. 6a), ~12 to 20 Å wide and parallel to the (1 3 1) plane. In these bands generated by intermolecular C–H···N contacts two hydrogen bonding motifs are visualized (Fig. 6a), R_2^2 (20) (B in Fig. 6a) and R_6^6 (38) (C). Analogies go still further, since in **2** also appear the 2D arrays build up by a parallel stacking of planes (Fig. 6b). The interplanar spacing, 3.66 Å (d(131)), the π···π interactions, T4b(1,2,3), and the RMS deviations from the planes defined by C and N atoms, 0.22 Å, again suggest delocalized electronic density clouds of the aromatic π···π bonds, as discussed above for **1**. Besides of this partial graphitic behaviour, certain C–H···O (T3b(6,7)) and C–H···π (T3b(8,9)) interactions help to stabilize the structure and can be used to explain in the same way the rotational torsions of the rings. As an special example it is convenient to mention the important contribution of a CH(methyl)/π(4-pyridyl) contact to the torsion of ring 3 (T3b(9), Fig. 5b). A similar involvement of the methyl H atoms, also detected in **1** (as indicated above), have been informed elsewhere [23], though all remaining contributions to this torsion, (for example those deriving from the H-bond donor capacity of ring 3 (T3b(8)), should be taken into account to get the final stabilized structure.

Finally, in this comparative study of the monomer vs. polymer, it should be noted that the bonding Zn–N(pyridyl) distances in **1** (Zn1–N11: 2.2505 (13) Å) and **2** (Zn1–N11: 2.2182 (12) Å) are reasonably close, but the Zn–N(pyrimidinyl) distance in polymer **2** (Zn1–N41: 2.3860 (13) Å) is significantly longer in comparison with those Zn–N(pyridyl) [24]. A partial explanation to the weakening of the Zn–N(pyrimidinyl) bond could be attributed to a more strong tendency of the pyrimidinyl rings to be stacked in comparison with the pyridyl ones: with more electron withdrawing nitrogen atoms in the rings the stacking interactions are intensify [25]. This effect is observed in complex **2** where both faces of the pyrimidinyl ring are involved in stacking interactions (T4b(2,3)) and,

on the other hand, in the coordinated pyridyl group this kind of interactions are insignificant.

4. Conclusions

The new hybrid terpyridine–pyrimidine ligand **L1** was synthetized and then characterized through spectroscopic methods. The coordinating properties of **L1** were tested by reacting with Zn(acac)$_2$ to give unexpectedly a mixture of the mononuclear complex **1** and the coordination polymer **2**. The hybrid ligand acting monodentaly uses the N atom from an exo-pyridyl group, but when acting as a bidentate-bridging ligand it uses two different N-donors: an exo-pyridyl group in alliance with a pyrimidinyl one. The N atom of the central pyridine ring in **L1** does not participate in the binding to the metal centers. The supramolecular structures of **1** and **2** can be understood considering the key role of the non-covalent C–H···N interactions that produce 2D substructures, which in combination with the π···π contacts provided by the abundant aromatic rings, develops the 3D arrangement. These synthons act in conjunction with several CH/O and CH/π hydrogen bonds to assemble the crystal packing.

References

[1] E.C. Constable, Chem. Soc. Rev. 36 (2007) 246–253.
[2] I. Eryazici, Ch.N. Moorefield, G.R. Newkome, Chem. Rev. 108 (2008) 1834–1895.
[3] U.S. Schubert, A. Winter, G.R. Newkome, Terpyridine-Based Materials, Wiley-VCH, Weinheim, 2011.
[4] J. Yoshida, S.-I. Nishikiori, R. Kuroda, Chem. Lett. 36 (5) (2007) 678–679.
[5] B.-C. Wang, Q.-R. Wu, H.-M. Hu, X.-L. Chen, Z.-H. Yang, Y.-Q. Shangguan, M.-L. Yang, G.-L. Xue, CrystEngComm 12 (2010) 485.
[6] D.-Y. Ma, D.-E. Sun, G.-Q. Li, Acta Crystallogr. Sect. E 67 (2011) m913.
[7] J. Song, B.-C. Wang, H.-M. Hu, L. Gou, Q.-R. Wu, X.-L. Yang, Y.-Q. Shangguan, F.-X. Dong, G.-L. Xue, Inorg. Chim. Acta 366 (2011) 134.
[8] C. Liu, Y.-B. Ding, X.-H. Shi, D. Zhang, M.-H. Hu, Y.-G. Yin, D. Li, Cryst. Growth Des. 9 (2009) 1275.
[9] E.C. Constable, G. Zhang, C.E. Housecroft, J.A. Zampese, CrystEngComm 13 (2011) 6864.
[10] J. Heine, J. Schmedt auf der Günne, S. Dehnen, J. Am. Chem. Soc. 133 (2011) 10018.
[11] K.-R. Ma, F. Ma, Y.-L. Zhu, L.-J. Yu, X.-M. Zhao, Y. Yang, W.-H. Duan, Dalton Trans. 40 (2011) 9774.
[12] G.R. Hanan, J. Wang, Synlett 8 (2005) 1251.
[13] Oxford Diffraction, CrysAlis PRO, version 171.33.48. Oxford Diffraction Ltd, Abingdon, Oxfordshire, England, 2009.
[14] G.M. Sheldrick, Acta Cryst. A 64 (2008) 112–122.
[15] A.L. Spek, PLATON, A Multipurpose Crystallographic Tool, Utrecht University, Utrecht, The Netherlands, 2005.
[16] C.F. Macrae, I.J. Bruno, J.A. Chisholm, P.R. Edgington, P. McCabe, E. Pidcock, L. Rodriguez-Monge, R. Taylor, J. van de Streek, P.A. Wood, J. Appl. Cryst. 41 (2008) 466–470.
[17] M.C. Etter, Acc. Chem. Res. 23 (1990) 120–126.
[18] J. Bernstein, R.E. Davis, L. Shimoni, N.L. Chang, Angew. Chem. Int. Ed. Engl. 34 (1995) 1555–1573.
[19] B.F. Minaev, G.V. Baryshnikov, A.A. Korop, V.A. Minaeva, M.G. Kaplunov, Opt. Spectrosc. 113 (2012) 298.
[20] V.A. Minaeva, B.F. Minaev, G.V. Baryshnikov, T.N. Kopylova, R.M. Gadirov, N.S. Eremina, Russ. J. Gen. Chem. 81 (2011) 2332.
[21] G.V. Baryshnikov, B.F. Minaev, A.A. Korop, V.A. Minaeva, A.N. Gusev, Russ. J. Inorg. Chem. 58 (2013) 928.
[22] B.F. Minaev, G.V. Baryshnikov, A.A. Korop, V.A. Minaeva, M.G. Kaplunov, Opt. Spectrosc. 114 (2013) 30.
[23] M.K. Milčič, V.B. Medaković, D.N. Sredojević, N.O. Juranić, S.D. Zarić, Inorg. Chem. 45 (2006) 4755.
[24] J.-F. Sun, G.-G. Hou, X.-P. Dai, Acta Cryst. E68 (2012) m91.
[25] R.R. Choudhury, R. Chitra, CrystEngComm 12 (2010) 2113.